ACS SENSORS

pubs.acs.org/acssensors

Article

Smartphone-Based High-Throughput Fiber-Integrated Immunosensing System for Point-of-Care Testing of the SARS-CoV-2 Nucleocapsid Protein

Ze Wu,[#] Cong Wang,[#] Bochao Liu, Chaolan Liang, Jinhui Lu, Jinfeng Li, Xi Tang, Chengyao Li,* and Tingting Li*

Cite This: https://doi.org/10.1021/acssensors.2c00754

Read Online

ACCESS | Metrics & More | Article Recommendations | Supporting Information

ABSTRACT: To control the coronavirus disease 2019 (COVID-19) pandemic, there is an urgent need for simple, rapid, and reliable detection methods to identify severe acute respiratory syndrome coronavirus 2 (SARS-CoV-2) infection, especially in community hospitals or clinical centers. The SARS-CoV-2 nucleocapsid protein (NP) is an important index for diagnosis of COVID-19. Here, we proposed a smartphone-based high-throughput fiber-integrated immunosensing system (HFIS) for detecting the SARS-CoV-2 NP in serum samples within 45 min. For the testing of NP standards, the linear detection range was 7.8−1000 pg/mL, the limit of detection was 7.5 pg/mL, and the cut-off value was 8.923 pg/mL. Twenty-five serum samples from clinically diagnosed COVID-19 patients and 100 negative control samples from healthy blood donors were tested for SARS-CoV-2 NP by HFIS, and the obtained results were compared with those of ELISA and Simple Western analysis. The results showed that the HFIS sensitivity and specificity were 72% [95% confidence interval (CI): 52.42−85.72%] and 100% (95% CI: 96.11−100%), respectively, which significantly correlated with those from the commercial ELISA kit and Simple Western analysis. This portable high-throughput HFIS assay could be an alternative test for detecting SARS-CoV-2 NP in blood samples on site.

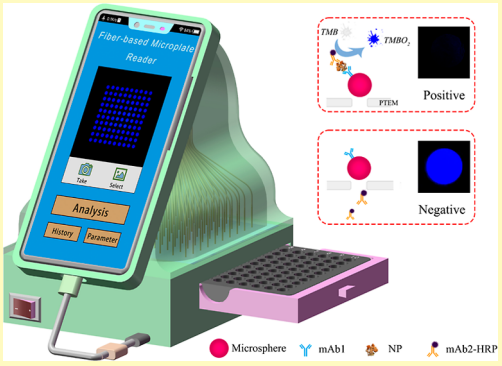

KEYWORDS: *SARS-CoV-2 nucleocapsid protein, high-throughput detection, smartphone, track-etched membrane, optical fiber*

COVID-19 pandemic caused by severe acute respiratory syndrome-related coronavirus 2 (SARS-CoV-2) is continuing to have a profound negative impact on our lives and may exist for a long time in the population.[1] The experience on pandemic prevention has proved that it can be effectively controlled by early screening and timely isolation of virus-infected individuals.[2,3] Currently, a large number of rapid detection methods for COVID-19 have been proposed, including the viral nucleic acid test,[4] immunological IgG/IgM tests, and antigen detection.[5,6] Some of them have already been used for practical diagnosis of SARS-CoV-2 infection.[7] So far, the reverse transcription polymerase chain reaction (RT-PCR) for detecting the viral nucleic acid from respiratory secretions has been widely used in clinical and has now become the gold standard for SARS-CoV-2 detection due to its high sensitivity.[8] However, RT-PCR also has some inherent defects, such as complicated and time-consuming operations and reliance on large instruments.[9,10] The serological immunochromatographic assay for IgG/IgM is also commonly used for rapid screening of SARS-CoV-2 infection owing to its advantages of being fast, having a low cost, and is independent of the need for instruments.[11,12] However, there is a window period infection (1−2 weeks) prior to antibody presence in the serum after exposure to virus, which makes serological antibody detection not suitable for early infection.[13] Due to the early occurrence time and a long window period, the direct detection of viral antigen has a potential advantage for diagnosis in the early course of COVID-19. The nucleocapsid protein (NP) is an important component of SARS-CoV-2,[14] which currently attracts more and more attention for its use in the development of detection methods.[15] Previously reported antigen detection methods were featured by the low cost and time saving process, but most of them were not sensitive enough, cumbersome, and required additional detection equipment.[13] They could not be widely implemented in resource-poor areas or developing countries. Therefore, there is an urgent and tremendous demand for low-cost, high-throughput, and instrument-independent assays for detection of SARS-CoV-2 antigens, which will be beneficial to an instant

Received: April 9, 2022
Accepted: June 15, 2022

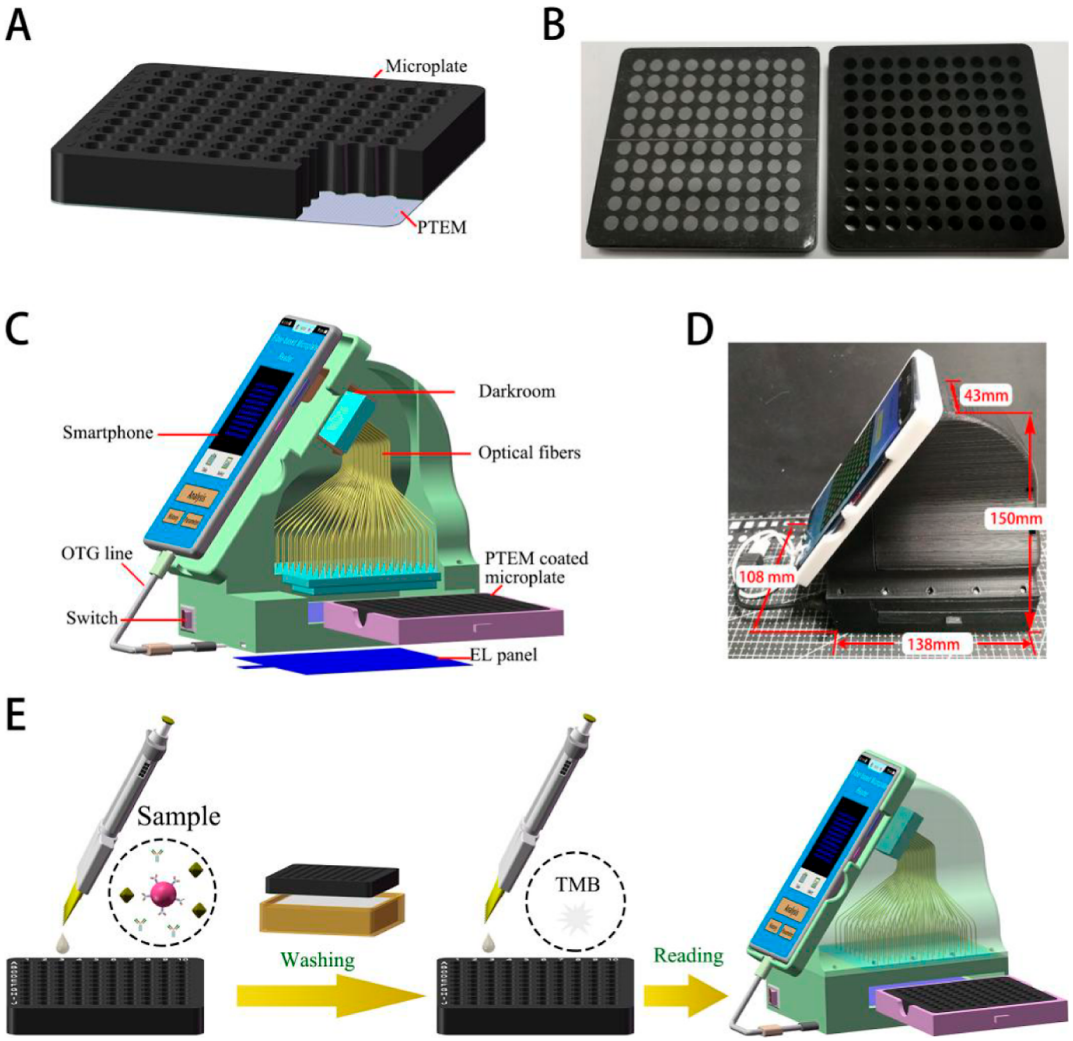

Figure 1. Design and assembly of the device of smartphone-based HFIS. (A) Structure of the PTEM-coated microplate. (B) Physical picture of both sides of the PTEM-coated microplate. (C) Blueprints of the handheld microplate reader device. (D) Physical drawing of the device. (E) Work flow chart of the smartphone-based HFIS.

and economical point-of-care testing in community hospitals or clinical centers.[16]

Enzyme-linked immunosorbent assay (ELISA) is one of the most commonly used low-cost and high-throughput methods for screening of the NP[17] but not suitable for on-site detection due to its complex process and reliance on professionals and special equipment. In order to simplify this assay, a porous washing system with the immunomagnetic bead technology was reported. The selective filtration of immunoglobulin-coupled microspheres was carried out using a multicapillary glass plate for quickly separating unrelated substances in the reaction.[18] However, the use of a multicapillary glass plate was complex, easy to damage, and high cost, which limited its large-scale application. Polycarbonate track-etched membrane (PTEM) was a membrane with high strength, low adsorption, and high filtration performance, which could be used to replace the multicapillary glass plate.[19] PTEMs were formed by preirradiation of polymer films with charged ions,[20] and were extensively used for ultrafiltration and purification,[21,22] while in the field of diagnosis, their application was explored for sensors.[23] In addition, to avoid relying on expensive instruments as used in ELISA, studies on reading of results were attempted.[24,25] The transmitted light from a microwell plate was imaged using the camera of a smartphone and then the image was analyzed. The method had obvious defects, for example, after the parallel light passed through the microplate, the optical signal at the edges had uncontrollable distortion and attenuation when captured, which led to great differences in the detection results between the edge and center wells. In order to deal with this situation, a microplate reading method gathering light together for capturing analysis was proposed.[26] This practical and creative idea solved the problem of interpreting the results from a cellphone-based microplate reader, but the light source of the device was an array composed of 24 lamp beads, which generated a lot of heat when used. Additionally, the light intensity generated by each individual lamp bead might not be guaranteed to be consistent. The light input of the quartz fiber used for light collection was low and difficult to process. It is still unable to avoid the insufficient sensitivity and the Hook effect false negatives due to an inappropriate ratio of antigen to antibody of ELISA itself as well.[27] Therefore, it is particularly critical to develop a new platform with a high-throughput, high sensitivity, low reagent consumption, and easy operation. To mitigate these problems, a novel optical fiber-based detection method was applied for

https://doi.org/10.1021/acssensors.2c00754
ACS Sens. XXXX, XXX, XXX−XXX

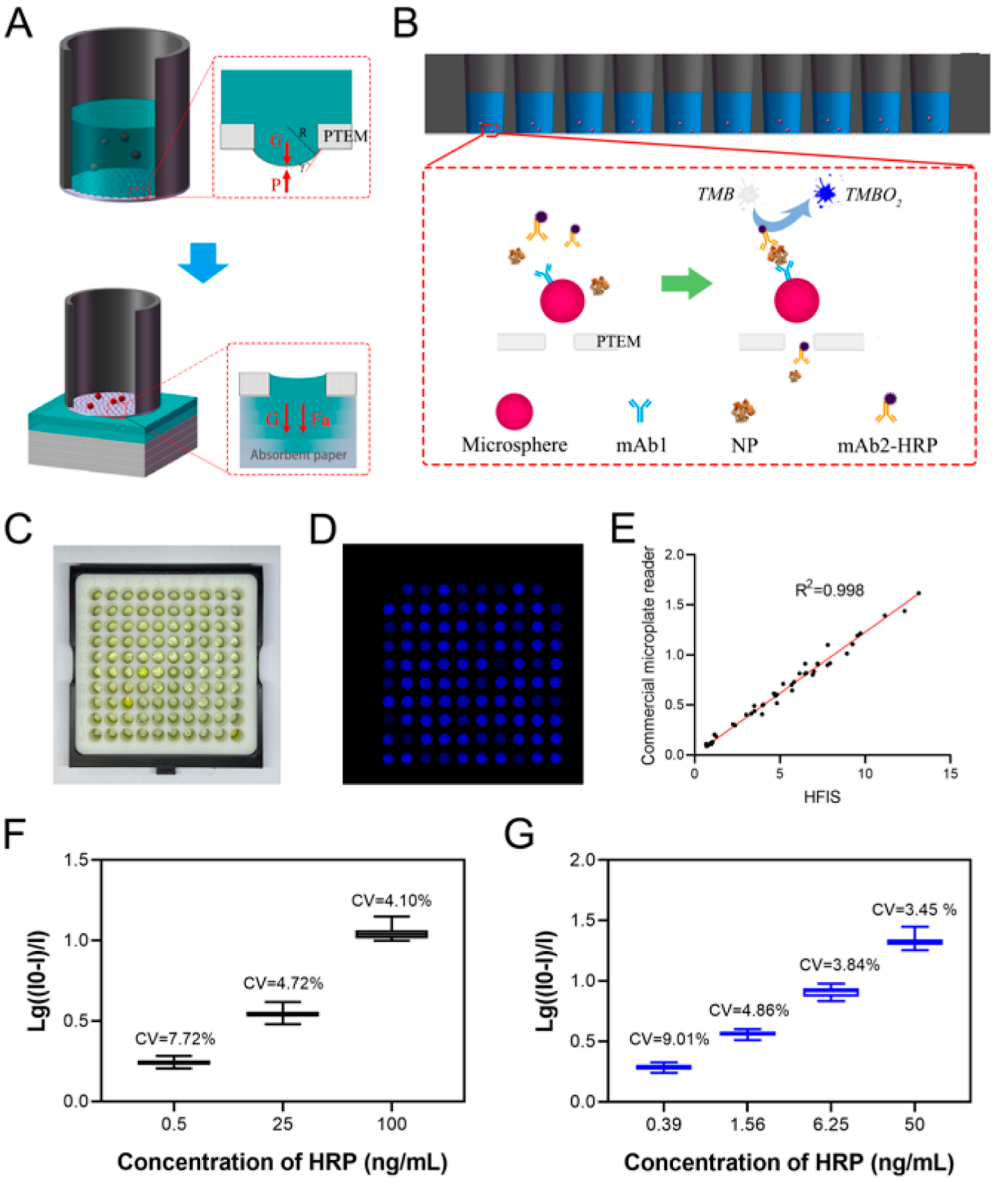

Figure 2. Principle and performance of HFIS. (A) Stress analysis of liquid on PTEM during use. (B) Principle of immunoassay in the PTEM-coated microplate. (C) Photograph of the PTEM-coated microplate after adding the chromogenic substrate. (D) Image of optical fiber ends captured by the smartphone. (E) Reading results from the optical fiber-based microplate reader compared with those of conventional microplate reader. (F) Intra-assay variation. (G) Inter-assay variation. The data represent the means ± SD of three independent tests.

the detection of SARS-CoV-2-neutralizing antibody in our laboratory.[28]

Here, an improved smartphone-based high-throughput fiber-integrated immunosensing system (HFIS) was proposed. The HFIS included a PTEM-based high-throughput immunoassay platform and a bundle of optical fiber-based handheld microplate reader. The PTEM-coated 100-well microplate was used as the container of immunoassay, the immunoglobulin-coupled microspheres were used as the reaction vehicle or vector, and the washing process was carried out using an absorbent paper. The application of PTEM greatly simplified the operation steps of immunoassay and shortened the procedure to less than 45 min, while the traditional ELISA needs more than 2 h. For realizing on-site detection, a smartphone-based optical fiber-integrated microplate reading device was manufactured, and the relevant application was designed. The electroluminescent (EL) panel was used to replace the lamp beads as the light source, and the poly(methyl methacrylate) (PMMA) optical fibers were used for light transmission and collection, so that the produced reading device had better stability and result reliability. By using a smartphone, the detection results could be uploaded to the terminal in real time, and the result analysis feedback and necessary medical guidance could be reported instantly. The whole process could make telemedicine possible and reduce the risk of cross infection of patients visiting hospital. This newly established platform has the advantages of high-throughput, high sensitivity, low cost, and easy operation and can be more easily applied in the field of point-of-care detection.

RESULTS AND DISCUSSION

Assembly and Application Process of the HFIS. The HFIS was mainly composed of two parts: a microplate with a

https://doi.org/10.1021/acssensors.2c00754
ACS Sens. XXXX, XXX, XXX−XXX

PTEM for the immunoassay and a handheld optic fiber bundle-integrated reading device for optical signal transmission and collection. The PTEM was tightly attached to the bottom of a 3D-printed 100-well microplate through a waterproof glue (Figure 1A). The outer square size of the 100-well microplate was 96 mm * 96 mm * 12 mm, the square area of wells was 82 mm * 82 mm * 12 mm, 100 wells with a diameter of 6.5 mm each were arranged in an array, and the wells with a midpoint spacing of 8.05 mm each were distributed (Figure 1B). In order to read and analyze the results from array detection, a portable microplate reader was designed and manufactured. It was mainly composed of a 100 mm * 100 mm EL panel, 100 PMMA optical fibers with a diameter of 1.1 mm each, a smartphone bracket frame, and a shell support (Figure 1C). The external dimension of the device was about 108 mm * 158 mm * 150 mm (Figure 1D). The raw material cost for manufacturing the device is as low as $10, and a single use cost is about $1 (similar to the cost of ELISA) (Table S1). Instead of the commonly used light-emitting diode (LED) or laser, a large-area inorganic EL flat panel was chosen as the light source, which formed a larger light-emitting area, but its more uniform light emission made heat generation difficult (Figure S1). Portable microplate readers have always been a research hotspot, but the principle of a microplate reader based on a smartphone reported in the literature is basically to take pictures directly after light passes through the microplate and then analyze the images. In order to solve the problem of a long imaging distance and edge distortion of the image, we tried to concentrate the transmitted light from each well to a dense area through individual optical fibers. At present, the widely used optical fibers are common glass fibers and polymeric optical fibers (POFs).[29,30] It is difficult to customize glass fibers due to its easy to break property and lack of light transmittance, while the PMMA fiber, a main type of POF, utilized in this study has easily customized diameters, better flexibility, and stronger light transmittance (Figure S2). A square area (82 mm * 82 mm) of 100 microwells within the plate was used for imaging, and the light signals were gathered in the 14 mm * 14 mm area through optical fiber transmission (Figure S3), which greatly reduced the focal length of shooting and effectively improved the shooting quality.

In order to achieve the need for large-scale on-site testing, the process should be simple and independent of the need for large instruments. In our study, the multiple steps of incubation and washing in conventional immunoassays were further reduced or simplified using a PTEM-coated microplate in our study. In practice, the users just need to add the serum or plasma sample to react with reagents in the PTEM-coated microplate and then keep the plate on the absorbent paper to filter the supernatant automatically. After washing the microplate twice with 0.05% Tween-20 phosphate-buffered saline (PBST), the substrate was added and the plate was let to stand for 15 min, and the reaction was terminated by adding 50 μL of 2 M hydrochloric acid (HCL). Finally, the results were read directly using a smartphone (Figure 1E). This biosensor was able to test up to 100 samples (including a negative control) within 45 min in a round and perform the real-time interpretation of results from the smartphone, which is very suitable for large-scale screening and point-of-care testing of COVID-19 or other infectious diseases in resource-limited areas.

Working Principle and Performance of HFIS. The polystyrene microspheres (PMs, 5 μm) are larger than the micropores of PTEM (approximately 3 μm) and therefore cannot pass through the PTEM-sealed microplate (Figure S4). In the reaction wells (Figure 2A), the solution will not flow out of the PTEM-bottomed microplate because of the Laplace pressure ($P = 2\gamma/R$, where R is the curvature radius of the meniscus and γ is the surface tension).[18] The solution in the PTEM-coated microplate can be maintained without leakage for 30 min at 37 °C (Figure S5A). Once the PTEM-coated microplate is placed on the absorbent paper, the Laplace pressure is disrupted, then 200 μL of reacting solution is filtered through PTEM of the microplate within 30 s by the gravity force (G) and the absorbing force (F_a) (Figure S5B). Thus, it is convenient to use the PTEM as a filter for the solid−liquid separation.

By using the PTEM-coated microplate for the immunoassay, a mixture of monoclonal antibody 1-labeled PMs (PMs-mAb1), targeting antigen (NP), and horseradish peroxidase (HRP)-labeled monoclonal antibody 2 (mAb2-HRP) is first added to the microwell. Under the action of Laplace pressure, the mixed solution is trapped in the PTEM-coated microplate, and the structural complexes of PMs-mAb1-NP-mAb2-HRP are formed within 30 min by an immunoreaction (Figure 2B). After placing the microplate on the absorbent paper, the unbound antibodies, free proteins, or unrelated materials are filtered through the PTEM-sealed microplate except for PMs-mAb1 or complexes. Finally, after washing the plate twice with PBST, the substrate solution [3,3′,5,5′-tetramethylbenzidine (TMB)] is added to the well for HRP reaction and color development. The results can be read using a handheld optical fiber-integrated reading device; the higher the concentration of the target protein in the sample, the stronger the color of the substrate developed in the well, and the less the light transmitted through the substrate (450 nm) to the smartphone camera via the optical fiber. The transmitted light is captured by the camera as the light spot. If the intensity of the light spot from the sample well is weaker than that from the negative control well, it indicates that the sample contains the targeting antigen (NP); if the light intensity from the sample well is the same as that of the negative control well, it suggests that the sample has no NP.

To evaluate the performance of the smartphone-based HFIS, we first verified the feasibility of reading results by a custom-designed APP. First, 90 μL of TMB solution was added to 100-well PTEM-coated microplates, subsequently 10 μL of different concentrations of HRP was added and the microplate was let to stand for 15 min at 37 °C, and finally 50 μL of termination solution was added; the reacted microplate was then put into the device connected with the smartphone to read results. Meanwhile, the reacted microplate was read using a conventional microplate reader. The results from the smartphone-based HFIS were consistent with those from the conventional microplate reader (Figure 2C,D), and the correlation coefficient is 0.998 (Figure 2E).

In addition, to determine the stability and repeatability of the HFIS, we analyzed the intra- and interbatch variations of sensing devices. For intrabatch evaluation, a panel of 100 identical samples was detected from a 100-well PTEM-coated microplate containing low, medium, and high concentrations of HRP. The results showed that the coefficient of variation (CV) values of the intra-batch reactions ranged from 4.10 to 7.72% (Figure 2F). For interbatch evaluation, 20 different batches of sensing devices were tested for the detection of the identical samples at four concentrations of HRP in the PTEM-

https://doi.org/10.1021/acssensors.2c00754
ACS Sens. XXXX, XXX, XXX−XXX

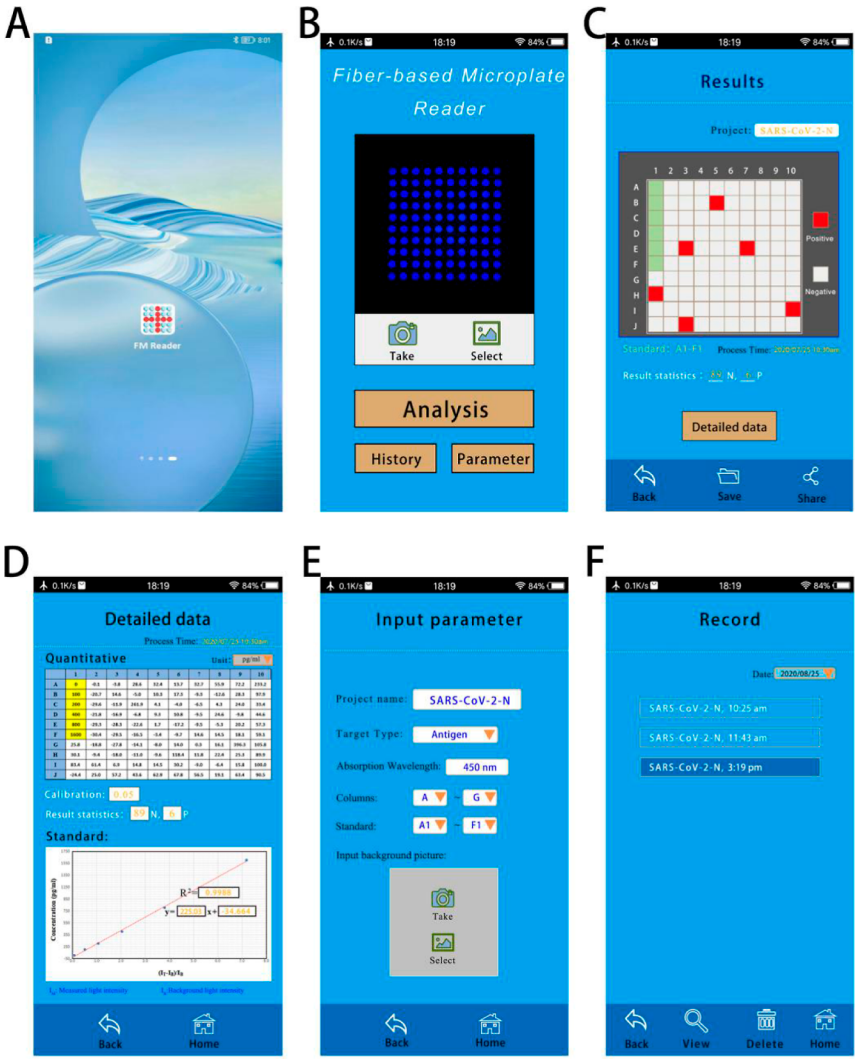

Figure 3. Screenshots of the *FM Reader* APP interface. (A) Designed APP software icon, named the *FM Reader*. (B) Main menu with user options and preview of captured images. (C) Color block diagram of negative/positive results appears after the user clicks the *Capture* icon to obtain the image and pressed the "*Analysis*" option. (D) Statistical analysis of the results and time at the bottom of diagram. Clicking the "Detailed data" option below, the statistical table at the top of a new interface displays the calculated NP concentration in each well and provides the standard curve and linear equation below. (E) "Input parameter" page for adding the parameters necessary to run the APP. (F) Record page displaying the submitted and processed tests with the time and test type.

coated microplate. The inter-CV values ranged from 3.45 to 9.01% (Figure 2G). These results showed that both intra- and inter-CV values were <10%, suggesting that HFIS had very good stability or repeatability.

Design of Smartphone Application (APP) for Data Processing. In order to achieve the quantitative analysis of target antigens, a custom-designed APP based on an Android environment, designated as a fiber-based handheld microplate reader (FM Reader), was developed, in which photography, image processing, and data analysis were integrated. It was installed and tested on a Huawei Mate 20 Pro smartphone running on Android 10.0.1. The main function of the FM Reader APP was to photograph the circular cross sections of the upper end bundle of optical fibers, calculate the optical darkness ratio (ODR) of the digital image of each light spot, and fit the calibration equation through different concentrations of NP standard and the corresponding ODR value. By using the ODR value corresponding to the tested sample and calibration equation, the results were displayed directly on the smartphone interface. ODR was calculated using formula 1

$$\mathrm{ODR} = (I_B - I_T)/I_B \quad (1)$$

where I_B is the average gray value of backgrounds and I_T is the average gray value of reaction wells. For each pixel, the gray value was calculated using formula 2

$$I = 0.1R + 0.09G + 0.81B \quad (2)$$

where I represents the gray value of the pixel and R, G, and B refer to the pixel intensity of red, green, and blue color channels, respectively.

Figure 3 shows the screenshots of the APP interface on the smartphone for imaging and analysis. A simple pattern is designed as the icon of the FM Reader (Figure 3A). The APP starts to run on the smartphone, and the main interface including the image and function area is entered after the user clicks on the *FM Reader* icon. A picture can be captured or selected from the smartphone album on the image box, and the function area includes three options: *Analysis*, *History*, and *Parameters* (Figure 3B). When the "*Analysis*" option is chosen, the negative/positive results of the sample in the microwell will

https://doi.org/10.1021/acssensors.2c00754
ACS Sens. XXXX, XXX, XXX−XXX

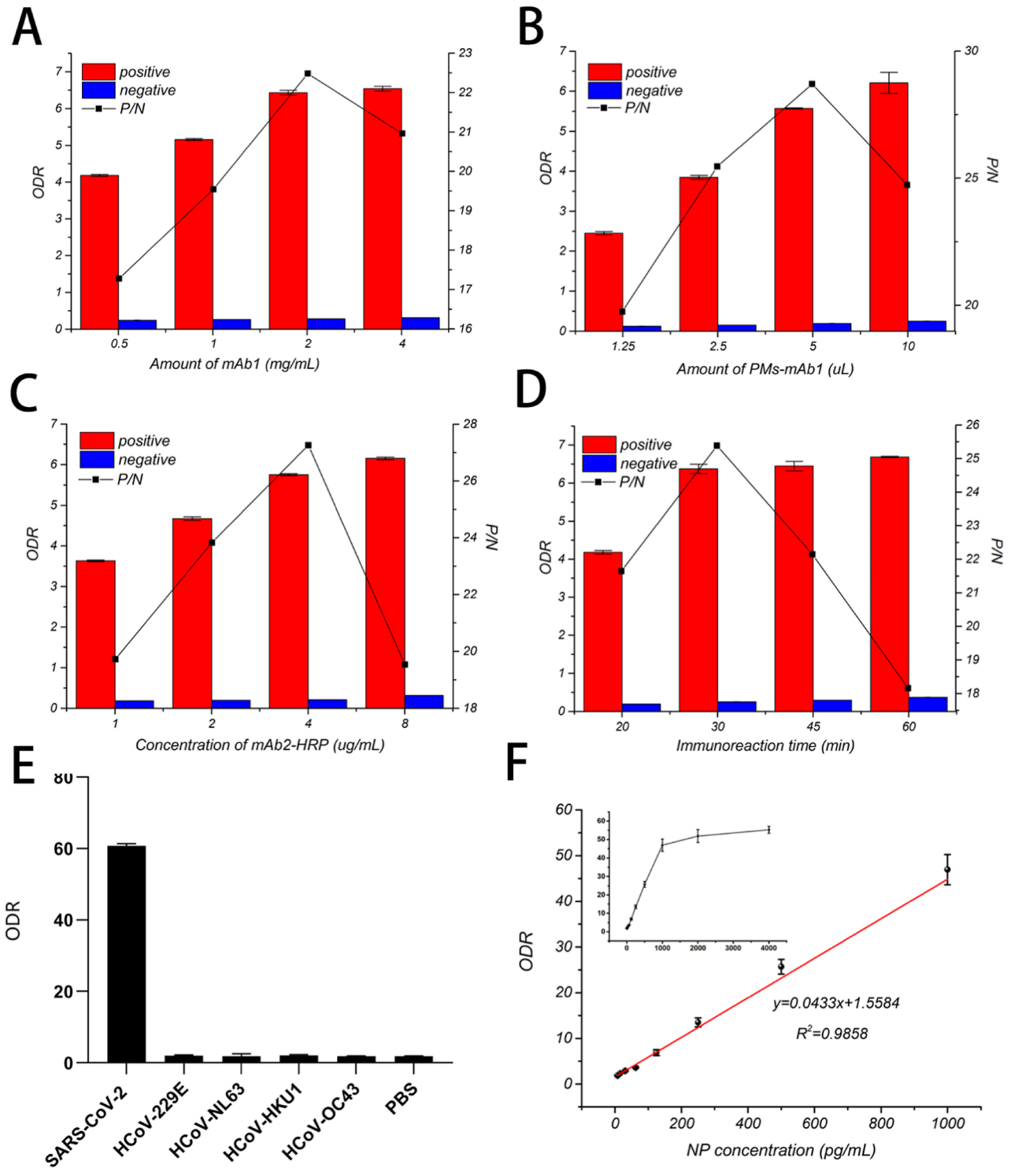

Figure 4. Optimization of working conditions of HIFS. Optimization of (A) the amount of mAb1 for labeling with PMs, (B) amount of PMs-mAb1, (C) amount of mAb1-HRP, and (D) immunoreaction time. (E) Specificity of HFIS was determined for reacting with 1 μg/mL coronavirus nucleocapsid proteins from SARS-CoV-2, HCoV-229E, HCoV-NL63, HCoV-HKU1, and HCoV-OC43 strains. PBS was used as negative control. (F) Standard curve for quantitative detection of SARS-CoV-2 NP by HFIS. The inset curve presents NP concentrations within 0−4000 pg/mL, of which the linear curve ranges within 0−1000 pg/mL. The data represent the means ± SD of three independent tests. ODR, the optical darkness ratio.

be visually displayed in gray/red color blocks, respectively. When the calculated concentration value is greater than the cut-off value, the sample is determined as positive (Figure 3C). The calculated concentration of the NP in the sample and the conversion formula will be displayed after clicking the "*Detailed data*" option on the interface (Figure 3D). After clicking the "*Parameter*" option in the main menu, the "Input parameter" page will pop up, for inputting the project name, test column position, background image, and so forth (Figure 3E). The "History" page appears after clicking the "*History*" option of

https://doi.org/10.1021/acssensors.2c00754
ACS Sens. XXXX, XXX, XXX−XXX

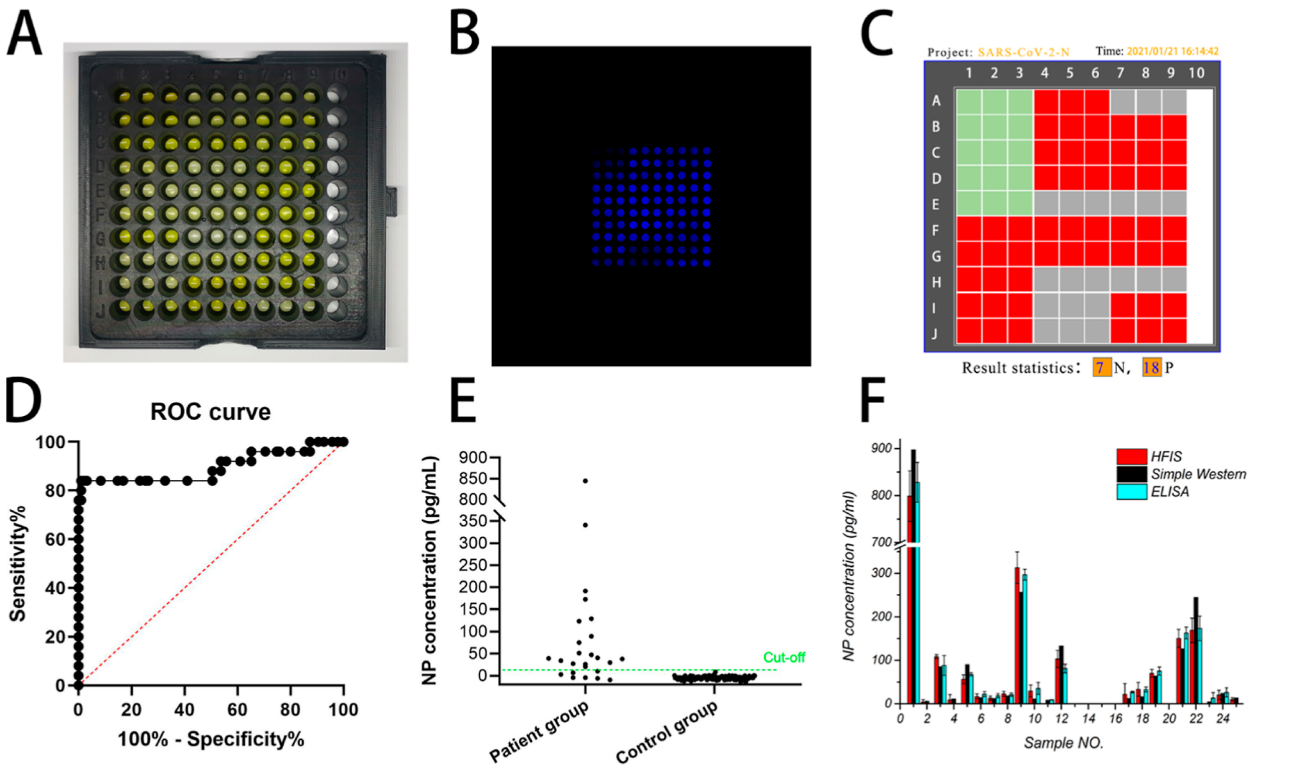

Figure 5. Testing of clinical samples by smartphone-based HFIS. (A) PTEM-coated microplate after immunoreaction. (B) Transmitted light image via optical fibers obtained by the smartphone camera. (C) Results of image analysis by the designed APP in the smartphone. (D) ROC curve of serum SARS-CoV-2 NP is plotted by GraphPad Prism 8, the area under the ROC curve is 0.8964, 95% confidence interval (CI) is 0.04898 to 0.9924, $P < 0.0001$, and the cut-off value is 8.923 pg/mL. (E) Detection of SARS-COV-2 NP in serum samples from 25 COVID-19 patients and 100 healthy blood donors. (F) Comparison of HFIS, Simple Western, and ELISA for quantification of NP in blood samples. The data represent the means ± SD of three independent tests.

the main menu and displays the submitted and processed tests on the server with the submission time and test type (Figure 3F).

Optimization of the Process and Testing of Standards. After designing the hardware and software of the sensing system, we optimized the detection process of the HFIS for negative PBS control (N) and positive NP standard (P) under different conditions. The optimal conditions were selected when the P/N value was the largest. The amounts of mAb1 for labeling with PMs (Figure 4A), PMs-mAb1 (Figure 4B), mAb2-HRP (Figure 4C), and the immunoreaction time (Figure 4D) were optimized in the reaction. To demonstrate specificity, the NPs from other coronavirus strains 229E, NL63, HKU1, and OC43 were tested by the HFIS (Figure 4E), showing no cross reaction in NPs between SARS-CoV-2 and other four human coronaviruses.

By using the HFIS, the quantification detection was performed for measuring NP standards (Figure 4F), and the limit of detection (LOD) was calculated by 3 × SD at 0 pg/mL divided by the slope of the calibration curve.[31] The linear detection range (LDR) was 7.8−1000 pg/mL and LOD was 7.5 pg/mL, while ELISA LDR and LOD were 15.6−1000 pg/mL or 13.5 pg/mL, respectively (Figure S6). Compared with ELISA, the HFIS had a wider detection range and higher sensitivity.

Quantitative Analysis of the NP in Serum Samples. Based on the aforementioned results, the developed smartphone-based HFIS can be used for quantitative analysis of the NP. Images from this proof-of-concept assay approach were captured and analyzed using a smartphone (Figure 5A−C). The cut-off value of HFIS was defined as 8.923 pg/mL (Figure 5D). The serum or plasma samples from 25 COVID-19 patients and 100 healthy blood donor controls were tested by HFIS (Figure 5E), ELISA (Figure S7), and Simple Western (Figure S8). The NP concentrations detected from COVID-19 patients varied insignificantly between HFIS and ELISA or Simple Western analysis (Figure 5F), indicating a good consistency between three assays. The sensitivity and specificity of HFIS were 72% (95% CI: 52.42−85.72%) and 100% (95% CI: 96.11−100%), respectively (Table 1). Samples no. 11 and 23 were detected only by Simple Western (Table S2), whose NP concentrations were, respectively, 8 and 4 pg/mL lower than the cut off (8.923 pg/mL) of HFIS. However,

Table 1. Detection of NP in Clinical Samples by HFIS, Simple Western Analysis, and ELISA

	HFIS		Simple Western		ELISA	
	positive	negative	positive	negative	positive	negative
control group (n = 100)	0	100	0	100	0	100
patient group (n = 25)	18	7	20	5	17	8
sensitivity % (95% CI)[a]	72.0% (52.42−85.72%)		80.0% (60.87−91.14%)		64.0% (44.52−79.75%)	
specificity % (95% CI)[a]	100% (96.11−100.0%)		98.95% (94.28−99.95%)		100% (96.11−100.0%)	

[a]The data were statistically analyzed by GraphPad Prism 8.

https://doi.org/10.1021/acssensors.2c00754
ACS Sens. XXXX, XXX, XXX−XXX

HFIS had higher detection sensitivity than ELISA (Table 1), while 91.6% samples within 2 weeks after PCR-confirmed infection were detected positive for the NP by ELISA according to a previous publication.[32] Therefore, the proposed smartphone-based HFIS could be a sensitive, user-friendly, portable, and large instrument-independent assay for rapid detection of the NP in human blood.

CONCLUSIONS

COVID-19 pandemic has been going on for nearly 3 years, and several antigen assays have been developed,[31] of which some tests have been industrialized so far.[33] RT-PCR is more sensitive in picking up individuals with acute infection. Testing of antigen, on the other hand, is somewhat less sensitive for detecting patient's samples. However, the antigen positivity of rapid detection was largely consistent with the timing of virus presence in infected individuals, illustrating that antigenic testing could be used to determine whether there is a risk of virus transmission or not.[34,35] The novel tests should provide an alternative that is of urgent need, especially assays that are rapid, high-throughput, sensitive, and independent of large equipment. In this study, a smartphone-based HFIS was designed for the detection of SARS-CoV-2 NP. A 100-well PTEM-coated microplate was used for immunoreaction and signal generation, wherein the special properties of PTEM allowed us to carry out rapid incubation and washing steps of testing. The light signals were collected by optical fibers in a handheld device, the images were captured by the smartphone camera, and the data were analyzed and processed by the separately designed FM-Reader APP. The stable and uniform light emitted by the EL panel was transmitted through the high-efficiency PMMA fibers, thus presenting the optical stability and user-friendliness with this small and cost-effective device. In order to enable users to have a better experience, we designed a customer-required APP for image capture and data process and analysis. The designed APP can directly report the negative and positive results from the testing samples with different colors of substrate reaction. By using the manufactured sensor hardware and FM Reader APP, the detection process was optimized for measuring NP in blood samples. The LOD was as low as 7.5 pg/mL, which was more sensitive than the value of conventional ELISA. Finally, 25 serum samples from COVID-19 patients and 100 plasma samples from healthy blood donors were tested. Based on the cut-off value of 8.923 pg/mL, the sensitivity and specificity of HFIS were determined to be 72 and 100%, respectively. The HFIS had a lower cost than the Simple Western test and a faster operation than ELISA. In addition, all immunological analyses and data processing could be completed by a handheld device, and no other large-scale equipment and excessive operations were required. Moreover, a maximum of 100 samples could be tested in the PTEM-coated microplate within 45 min in a round, which could be used for a large-scale screening of NP in blood samples.

Some specific conditions are required for use of the HFIS system which may lead to additional costs, including the smartphone, internet, reagent storage at 4 °C, and 50 μL of sample volume. There is still room for improvement for this method, and the low cost and compact size of the HFIS can be conveniently used in community hospitals and clinical centers, or in the countryside in remote areas.

MATERIALS AND METHODS

Serum or Plasma Samples. COVID-19 patients' sera used in this study were provided by Shenzhen Center for Disease Control and Prevention (CDC), which were initially confirmed positive for SARS-CoV-2 RNA by RT-qPCR. Negative plasma controls were obtained from the Guangzhou Blood Center, which were collected from healthy blood donors during the period of May to October of 2019. All samples were inactivated for 40 min by heating at 56 °C. This study was approved by the Ethics Committee of Shenzhen CDC. All individuals involved in this study signed an informed consent.

Chemicals and Materials. Bovine serum albumin (BSA) and 3,3′,5,5′-tetramethylbenzidine (TMB) were purchased from Sigma (St. Louis, USA). *N*-Hydroxy-succinimide (NHS) and 1-(3-dimethylaminopropyl)-3-ethylcarbodiimide hydrochloride (EDC) were purchased from BBI Life Sciences (Shanghai, China). Streptavidin-conjugated horseradish peroxidase (SA-HRP) and NHS-biotin were purchased from Thermo Fisher Scientific (USA). Theblack-coated PMMA fiber (1.2 mm in diameter) was obtained from Shenzhen Chuangli Fiber Optic Material Co., Ltd. (Shenzhen, China). PTEMs were purchased from Beijing Tsingneng Chuangxin Science and Technology Co., Ltd. (Beijing, China), and the EL panel (450 nm) was purchased from Xinlong Lightwear (Shenzhen, China). Polystyrene microspheres (PMs, 5 μm in diameter) were purchased from Suzhou Beaver Biosciences Inc. (Jiangsu, China). The SARS-CoV-2 NP standard was purchased from Biodragon Immunotechnologies Co. Ltd. (Beijing, China), and the pair-matched monoclonal antibodies (5×10^4, 4G11) to NP were prepared in our laboratory.[36] The SARS-CoV-2 (2019-nCoV) Nucleocapsid Detection ELISA Kits were purchased from Biodragon Immunotechnologies Co. Ltd. (Beijing, China) for comparative assay for the detection of SARS-CoV-2-NP. NPs of coronavirus HCoV-229E, HcoV-NL63, HcoV-HKU1, and HcoV-OC43 strains were purchased from Sino Biological Inc. (Beijing, China) and used for testing of cross reactivity.

Design and Assembly of the PTEM-Coated Microplate. The PTEM-based microplate is designed as the immunoassay vessel. The complete microplate is composed of a 100-well microplate with its bottom sealed by the PTEM with a waterproof adhesive (Figure 1A). The 96 mm * 96 mm * 12 mm perforated microplate was made by UV-curing three-dimensional (3D) printing with an opaque photosensitive resin. Then, PTEM was stuck to the bottom of the microplate by the following processes (Figure 1B): (1) the side A of the waterproof double-sided adhesive was pasted to the bottom of the perforated microplate; (2) a punch was used to remove the double-sided adhesive tape corresponding to each well of the microplate; and (3) the isolation layer on the side B of double-sided adhesive tape was tore off, the PTEM was cut to a suitable size, and it was made flat (Figure S9). PTEM was soaked in the pretreatment reagent (0.01 M PBS and 1% BSA, pH 7.4) for 1 h to reduce non-specific adsorption, and before use a layer of hydrophobic reagent was sprayed on the outer bottom surface.

Design and Assembly of Optical Fiber-Based Handheld Microplate Reader. A specially designed optical fiber-based handheld microplate reader (FM Reader) was used for transmitting and capturing light signals (Figure 1C,D). It was mainly composed of a 100 mm * 100 mm EL panel, 100 poly(methyl methacrylate) (PMMA) optical fibers with a diameter of 1.1 mm each, a smartphone bracket frame, and a shell support. The EL was tiled at the bottom of the device, and the emission wavelength was 450 nm. All 100 fibers were cut to 150 mm in length, the cross sections of both ends were flattened by a fine sandpaper, and then polished with wax. One end of 100 individual optical fibers was fixed to a PVC platform board with glue corresponding to each well of the microplate. Another end of optical fibers was gathered to a 10 × 10 array in a small square hood facing the smartphone camera. The external structures of this device, including the smartphone bracket frame and the shell support, were fabricated by FDM 3D printing and then fitted with optical attachments.

Preparation of PMs-mAb1 and mAb2-HRP Conjugates. Five microliters of 1 mg/mL EDC and 5 μL of 2 mg/mL NHS were added

https://doi.org/10.1021/acssensors.2c00754
ACS Sens. XXXX, XXX, XXX−XXX

to 120 μL polystyrene microspheres (PMs) for 30 min incubation, and the excessive EDC and NHS were removed by centrifugation (12,000 rpm/min, 15 min). Forty microliters of certain concentration of mAb1 were mixed with PMs and incubated for 2 h at room temperature. Then, 200 μL of blocking buffer was added to block the surface of PMs. After 1 h incubation, PMs-mAb1 was washed by centrifugation at 3000 rpm for 5 min and resuspended in 300 μL of reconstitution buffer (10 mM PBS, 0.05% Tween-20, 5% sucrose, and 0.025% NaN_3, pH 7.4). mAb2-HRP conjugates were prepared by mixing the activated HRP and mAb2 in a 1:2 ratio, then the reaction solution was adjusted to pH 9.5 for incubating at 37 °C for 1 h, and finally adjusted to pH 7.0 for storage after adding 1.5 mg of sodium borohydride.

Detection of NP Standards by Sandwich Immunoassay. Fifty microliters NP standards diluted in 0.2% BSA at concentrations of 0, 0.015, 0.031, 0.0625, 0.125, 0.25, 0.5, and 1 ng/mL were added to the PTEM-coated microplate. A certain amount of PMs-mAb1 and 50 μL of a certain concentration of mAb2-HRP were added to each well of the microplate and incubated for 30 min at room temperature. The reactive solution in the microplate was removed by filtration with PTEM in contact with absorbent papers, washed twice with PBST, and then 100 μL of substrate solution was added to the PTEM-coated microplate. After 15 min of color development in the dark, 50 μL of 2 M HCL was added to the PTEM-coated microplate for termination of the reaction. The EL-emitted light (450 nm) was filtered through the reacted substrate to the FM Reader via individual optical fibers and then the transmitted light was captured and analyzed by the smartphone.

Detection of Clinical Samples by HFIS. Fifty microliters of undiluted serum or plasma samples from 25 COVID-19 patients and 100 blood donors were added to the PTEM-coated microplate. Then, 5 μL of PMs-mAb1 and 50 μL of 4 μg/mL mAb2-HRP were added to each well of the microplate and incubated for 30 min at room temperature for detection of NP using the above-described HFIS. All samples were tested, and the results obtained using the commercial ELISA kit and Simple Western analysis were compared.[37]

Statistical Analysis. Statistical analysis was carried out using the Graphpad Prism 8 software. LOD is calculated as follows: 3 × SD at 0 ng/mL divided by the slope of the calibration curve. LDR is the interval when the correlation coefficient (R^2) of the linear regression equation is the largest.

■ ASSOCIATED CONTENT

Supporting Information

The Supporting Information is available free of charge at https://pubs.acs.org/doi/10.1021/acssensors.2c00754.

Costs for HFIS and ELISA; quantitative detection of NP in blood from COVID-19 patients; comparison of LED lamp beads and the EL panel; comparison of the PMMA fiber and quartz fiber; area of the microplate for signal generation and the area of the 10 × 10array for photographing after light collection via optical fibers; SEM photographs; change of liquid in the PTEM-coated microplate during incubation and washing; detection of NP standards by ELISA; detection of NP standards by a commercial ELISA kit; quantitative analysis of NP in serum samples by Simple Western analysis; and preparation process of the PTEM-coated microplate (PDF)

■ AUTHOR INFORMATION

Corresponding Authors

Chengyao Li − *Department of Transfusion Medicine, School of Laboratory Medicine and Biotechnology, Southern Medical University, Guangzhou 510515, P. R. China*; Email: chengyaoli@hotmail.com

Tingting Li − *Department of Transfusion Medicine, School of Laboratory Medicine and Biotechnology, Southern Medical University, Guangzhou 510515, P. R. China*; orcid.org/0000-0001-5727-2179; Email: apple-ting-007@163.com

Authors

Ze Wu − *Department of Transfusion Medicine, School of Laboratory Medicine and Biotechnology, Southern Medical University, Guangzhou 510515, P. R. China; Department of Laboratory Medicine, Nanfang Hospital, Southern Medical University, Guangzhou 510515, P. R. China*; orcid.org/0000-0001-6422-532X

Cong Wang − *Department of Transfusion Medicine, School of Laboratory Medicine and Biotechnology, Southern Medical University, Guangzhou 510515, P. R. China*

Bochao Liu − *Department of Transfusion Medicine, School of Laboratory Medicine and Biotechnology, Southern Medical University, Guangzhou 510515, P. R. China; Guangzhou Blood Center, Guangzhou 510091, P. R. China*

Chaolan Liang − *Department of Transfusion Medicine, School of Laboratory Medicine and Biotechnology, Southern Medical University, Guangzhou 510515, P. R. China*

Jinhui Lu − *Department of Transfusion Medicine, School of Laboratory Medicine and Biotechnology, Southern Medical University, Guangzhou 510515, P. R. China*

Jinfeng Li − *Shenzhen Key Laboratory of Molecular Epidemiology, Shenzhen Center for Disease Control and Prevention, Shenzhen 518054, P. R. China*

Xi Tang − *Department of Infection, The First People's Hospital of Foshan, Foshan 528010, China*

Complete contact information is available at: https://pubs.acs.org/10.1021/acssensors.2c00754

Author Contributions

#Z.W. and C.W. contributed equally to this work. Z.W. and C.W. participated in the study design, analysis of data, and writing of the manuscript. Z.W. and C.W. performed the laboratory examination. B.L., C.L., J.L., J.L., and X.T. provided key materials. C.L. and T.L. analyzed data and revised the manuscript. All authors read and approved the final version of manuscript.

Notes

The authors declare no competing financial interest.

The authors declare that all data supporting the findings of this study are available within the article and its Supporting Information files can be obtained from the corresponding author upon reasonable request.

■ ACKNOWLEDGMENTS

The authors thank Shenzhen CDC for providing COVID-19 patients' serum samples and Guangzhou, Shenzhen, Harbin, Chengdu, and Xi'an Blood Centers for providing healthy blood donor samples. This study was supported by the grants from the National Natural Science Foundation of China (nos. 31970886, 31770185, and 81871655) and Guangdong Innovative and Entrepreneurial Research Team Program (no. 2014ZT05S123).

■ REFERENCES

(1) Ludwig, S.; Zarbock, A. Coronaviruses and SARS-CoV-2: A Brief Overview. *Anesth. Analgesia* **2020**, *131*, 93−96.

(2) Huang, L.; Ding, L.; Zhou, J.; Chen, S.; Chen, F.; Zhao, C.; Xu, J.; Hu, W.; Ji, J.; Xu, H.; Liu, G. L. One-step rapid quantification of

SARS-CoV-2 virus particles via low-cost nanoplasmonic sensors in generic microplate reader and point-of-care device. *Biosens. Bioelectron.* **2021**, *171*, 112685.
(3) Chang, Y.-F.; Wang, W.-H.; Hong, Y.-W.; Yuan, R.-Y.; Chen, K.-H.; Huang, Y.-W.; Lu, P.-L.; Chen, Y.-H.; Chen, Y.-M. A.; Su, L.-C.; Wang, S.-F. Simple Strategy for Rapid and Sensitive Detection of Avian Influenza A H7N9 Virus Based on Intensity-Modulated SPR Biosensor and New Generated Antibody. *Anal. Chem.* **2018**, *90*, 1861−1869.
(4) Corman, V. M.; Landt, O.; Kaiser, M.; Molenkamp, R.; Meijer, A.; Chu, D. K.; Bleicker, T.; Brünink, S.; Schneider, J.; Schmidt, M. L.; Mulders, D. G.; Haagmans, B. L.; van der Veer, B.; van den Brink, S.; Wijsman, L.; Goderski, G.; Romette, J.-L.; Ellis, J.; Zambon, M.; Peiris, M.; Goossens, H.; et al. Detection of 2019 novel coronavirus (2019-nCoV) by real-time RT-PCR. *Euro Surveill.* **2020**, *25*, 2000045.
(5) Qu, J.; Wu, C.; Li, X.; Zhang, G.; Jiang, Z.; Li, X.; Zhu, Q.; Liu, L. Profile of Immunoglobulin G and IgM Antibodies Against Severe Acute Respiratory Syndrome Coronavirus 2 (SARS-CoV-2). *Clin. Infect. Dis.* **2020**, *71*, 2255−2258.
(6) Wang, C.; Shi, D.; Wan, N.; Yang, X.; Liu, H.; Gao, H.; Zhang, M.; Bai, Z.; Li, D.; Dai, E.; Rong, Z.; Wang, S. Development of spike protein-based fluorescence lateral flow assay for the simultaneous detection of SARS-CoV-2 specific IgM and IgG. *Analyst* **2021**, *146*, 3908−3917.
(7) Mohit, E.; Rostami, Z.; Vahidi, H. A comparative review of immunoassays for COVID-19 detection. *Expet Rev. Clin. Immunol.* **2021**, *17*, 573−599.
(8) Li, Z.; Bai, Y.; You, M.; Hu, J.; Yao, C.; Cao, L.; Xu, F. Fully integrated microfluidic devices for qualitative.; quantitative and digital nucleic acids testing at point of care. *Biosens. Bioelectron.* **2021**, *177*, 112952.
(9) Li, J.; Lillehoj, P. B. Microfluidic Magneto Immunosensor for Rapid, High Sensitivity Measurements of SARS-CoV-2 Nucleocapsid Protein in Serum. *ACS Sens.* **2021**, *6*, 1270−1278.
(10) Braunstein, G. D.; Schwartz, L.; Hymel, P.; Fielding, J. False Positive Results With SARS-CoV-2 RT-PCR Tests and How to Evaluate a RT-PCR-Positive Test for the Possibility of a False Positive Result. *J. Occup. Environ. Med.* **2021**, *63*, e159−e162.
(11) Zhang, Z. L.; Hou, Y. L.; Li, D. T.; Li, F. Z. Diagnostic efficacy of anti-SARS-CoV-2 IgG/IgM test for COVID-19: A meta-analysis. *J. Med. Virol.* **2021**, *93*, 366−374.
(12) Pan, Y.; Li, X.; Yang, G.; Fan, J.; Tang, Y.; Zhao, J.; Long, X.; Guo, S.; Zhao, Z.; Liu, Y.; Hu, H.; Xue, H.; Li, Y. Serological immunochromatographic approach in diagnosis with SARS-CoV-2 infected COVID-19 patients. *J. Infect.* **2020**, *81*, e28−e32.
(13) Hingrat, Q. L.; Visseaux, B.; Laouenan, C.; Tubiana, S.; Bouadma, L.; Yazdanpanah, Y.; Duval, X.; Burdet, C.; Ichou, H.; Damond, F.; Bertine, M.; Benmalek, N.; Choquet, C.; Timsit, J. F.; Ghosn, J.; Charpentier, C.; Descamps, D.; Houhou-Fidouh, N. Detection of SARS-CoV-2 N-antigen in blood during acute COVID-19 provides a sensitive new marker and new testing alternatives. *Clin. Microbiol. Infect.* **2020**, *27*, 789.e1−789.e5.
(14) Zeng, W.; Liu, G.; Ma, H.; Zhao, D.; Yang, Y.; Liu, M.; Mohammed, A.; Zhao, C.; Yang, Y.; Ding, C.; Ma, X.; Weng, J.; Gao, Y.; He, H.; Jin, T. Biochemical characterization of SARS-CoV-2 nucleocapsid protein. *Biochem. Biophys. Res. Commun.* **2020**, *527*, 618−623.
(15) Diao, B.; Wen, K.; Chen, J.; Liu, Y.; Wu, Y. Diagnosis of Acute Respiratory Syndrome Coronavirus 2 Infection by Detection of Nucleocapsid Protein. **2020**, medRxiv 2020.03.07.20032524.
(16) Häuser, F.; Sprinzl, M. F.; Dreis, K. J.; Renzaho, A.; Youhanen, S.; Kremer, W. M.; Podlech, J.; Galle, P. R.; Lackner, K. J.; Rossmann, H.; Lemmermann, N. A. Evaluation of a laboratory-based high-throughput SARS-CoV-2 antigen assay for non-COVID-19 patient screening at hospital admission. *Med. Microbiol. Immunol.* **2021**, *210*, 165−171.
(17) Liu, W.; Liu, L.; Kou, G.; Zheng, Y.; Ding, Y.; Ni, W.; Wang, Q.; Tan, L.; Wu, W.; Tang, S.; Xiong, Z.; Zheng, S. Evaluation of Nucleocapsid and Spike Protein-Based Enzyme-Linked Immunosorbent Assays for Detecting Antibodies against SARS-CoV-2. *J. Clin. Microbiol.* **2020**, *58*, No. e00461-20.
(18) Chen, F.; Mao, S.; Zeng, H.; Xue, S.; Yang, J.; Nakajima, H.; Lin, J.-M.; Uchiyama, K. Inkjet nanoinjection for high-thoughput chemiluminescence immunoassay on multicapillary glass plate. *Anal. Chem.* **2013**, *85*, 7413−7418.
(19) Jain, B.; Kulkarni, S.; Banerjee, S.; Rajan, M. Microarray immunoassay for thyrotropin on track-etched membranes using radiotracers. *J. Radioanal. Nucl. Chem.* **2019**, *1*, 99.
(20) Apel, P. Track etching technique in membrane technology. *Radiat. Meas.* **2001**, *34*, 559−566.
(21) Kros, A.; Nolte, R. J. M.; Sommerdijk, N. A. J. M. Conducting polymers with confined dimensions: track-etch membranes for amperometric biosensor applications. *Adv. Mater.* **2002**, *14*, 1779−1782.
(22) Hanot, H.; Ferain, E. Industrial applications of ion track technology. *Nucl. Instrum. Methods Phys. Res., Sect. B* **2009**, *267*, 1019−1022.
(23) Koochaki, Z.; Higson, S. P. J.; Mutlu, M.; Vadgam, P. M. The diffusion limited oxidase-based glucose enzyme electrode: relation between covering membrane permeability and substrate response. *J. Membr. Sci.* **1993**, *76*, 261−268.
(24) Zhdanov, A.; Keefe, J.; Franco-Waite, L.; Konnaiyan, K. R.; Pyayt, A. Mobile phone based ELISA (MELISA). *Biosens. Bioelectron.* **2018**, *103*, 138−142.
(25) McGeough, C. M.; O'Driscoll, S. Camera phone-based quantitative analysis of C-reactive protein ELISA. *IEEE Trans. Biomed. Circuits Syst.* **2013**, *7*, 655−659.
(26) Berg, B.; Cortazar, B.; Tseng, D.; Ozkan, H.; Feng, S.; Wei, Q.; Chan, R. Y.-L.; Burbano, J.; Farooqui, Q.; Lewinski, M.; Di Carlo, D.; Garner, O. B.; Ozcan, A. Cellphone-Based Hand-Held Microplate Reader for Point-of-Care Testing of Enzyme-Linked Immunosorbent Assays. *ACS Nano* **2015**, *9*, 7857−7866.
(27) Fernando, S. A.; Wilson, G. S. Multiple epitope interactions in the two-step sandwich immunoassay. *J. Immunol. Methods* **1992**, *151*, 67.
(28) Wang, C.; Wu, Z.; Liu, B.; Zhang, P.; Lu, J.; Li, J.; Zou, P.; Li, T.; Fu, Y.; Chen, R.; Zhang, L.; Fu, Q.; Li, C. Track-etched membrane microplate and smartphone immunosensing for SARS-CoV-2 neutralizing antibody. *Biosens. Bioelectron.* **2021**, *192*, 113550.
(29) Peters, K. Polymer optical fiber sensors—a review. *Smart Mater. Struct.* **2011**, *20*, 013002.
(30) Mizuno, Y.; Theodosiou, A.; Kalli, K.; Liehr, S.; Nakamura, K. Distributed polymer optical fiber sensors: a review and outlook. *Photon. Res.* **2021**, *9*, 1719.
(31) Li, J.; Lillehoj, P. B. Microfluidic magneto immunosensor for rapid, high sensitivity measurements of SARS-CoV-2 nucleocapsid protein in serum. *ACS Sens.* **2021**, *6*, 1270−1278.
(32) Thudium, R. F.; Stoico, M. P.; Estrid, H.; Julie, H.; Krarup, H. B.; Larsen, M.; Madsen, P. H.; Nielsen, S. D.; Ostrowski, S. R.; Amanda, P. Early Laboratory Diagnosis of COVID-19 by Antigen Detection in Blood Samples of the SARS-CoV-2 Nucleocapsid Protein. *J. Clin. Microbiol.* **2021**, *59*, No. e0100121.
(33) My, A.; Ef, B.; Kgz, B. COVID-19 diagnosis—A review of current methods. *Biosens. Bioelectron.* **2021**, *172*, 112752.
(34) Corman, V. M.; Haage, V. C.; Bleicker, T.; Schmidt, M. L.; Mühlemann, B.; Zuchowski, M.; Jo, W. K.; Tscheak, P.; Möncke-Buchner, E.; Müller, M. A.; Krumbholz, A.; Drexler, J. F.; Drosten, C. Comparison of seven commercial SARS-CoV-2 rapid point-of-care antigen tests: a single-centre laboratory evaluation study. *Lancet Microbe* **2021**, *2*, e311−e319.
(35) Killingley, B.; Mann, A. J.; Kalinova, M.; Boyers, A.; Goonawardane, N.; Zhou, J.; Lindsell, K.; Hare, S. S.; Brown, J.; Frise, R.; Smith, E.; Hopkins, C.; Noulin, N.; Löndt, B.; Wilkinson, T.; Harden, S.; McShane, H.; Baillet, M.; Gilbert, A.; et al. Safety, tolerability and viral kinetics during SARS-CoV-2 human challenge in young adults. *Nat. Med.* **2022**, *28*, 1031.
(36) Liu, B.; Wu, Z.; Liang, C.; Lu, J.; Li, J.; Zhang, L.; Li, T.; Zhao, W.; Fu, Y.; Hou, S.; Tang, X.; Li, C. Development of a Smartphone-

https://doi.org/10.1021/acssensors.2c00754
ACS Sens. XXXX, XXX, XXX−XXX

Based Nanozyme-Linked Immunosorbent Assay for Quantitative Detection of SARS-CoV-2 Nucleocapsid Phosphoprotein in Blood. *Front. Microbiol.* **2021**, *12*, 692831.
(37) Nguyen, U.; Squaglia, N.; Boge, A.; Fung, A. P. The Simple Western: a gel-free, blot-free, hands-free Western blotting reinvention. *Nat. Methods* **2011**, *8*, v−vi.

https://doi.org/10.1021/acssensors.2c00754
ACS Sens. XXXX, XXX, XXX−XXX